Laser induced fluorescence in nanosecond repetitively pulsed discharges for CO_2 conversion

L. M. Martini[1], N. Gatti[1,3], G. Dilecce[2,1], M. Scotoni[1] and P. Tosi[1]

[1]Dipartimento di Fisica Università di Trento, Via Sommarive 14, 38123 Povo - Trento, Italy
[2]CNR NANOTEC - PLasMI Lab., via Amendola 122/D, 70126 Bari, Italy
[3]Dutch Institute for Fundamental Energy Research, P.O. box 6336, 5600 HH Eindhoven, The Netherlands

E-mail: `luca.martini.1@unitn.it`

Abstract. A CO_2 nanosecond repetitively pulsed discharge (NRP) is a harsh environment for laser induced fluorescence (LIF) diagnostics. The difficulties arise from it being a strongly collisional system in which the gas composition, pressure and temperature, have quick and strong variations. The relevant diagnostic problems are described and illustrated through the application of LIF to the measurement of the OH radical in three different discharge configurations, with gas mixtures containing CO_2+H_2O. These range from a dielectric barrier NRP with He buffer gas, a less hostile case in which absolute OH density measurement are possible, to an NRP in CO_2+H_2O, where the full set of drawbacks is at work. In the last case, the OH density measurement is not possible with laser pulses and detector time resolution in the ns time scale. Nevertheless, it is shown that with a proper knowledge of the collisional rate constants involved in the LIF process, a Collisional Energy Transfer (CET)-LIF methodology is still applicable to deduce the gas composition from the analysis of LIF spectra.

PACS numbers: 33.50.Dq, 33.50.Hv, 34.50.Ez, 52.80.Tn, 82.33.Xj

Keywords: Nanosecond Pulsed Discharge, Laser induced fluorescence, CO_2 conversion.

Submitted to: *Plasma Phys. Control. Fusion*

1. Introduction

The conversion of CO_2 by non-thermal plasma technology is gaining increasing interest due to a number of potential advantages, like working at room temperature with no switch-on inertia, or the possibility to get value-added products, like gaseous or liquid fuels, from carbon dioxide with the addition of a hydrogen source (e.g. H_2O [1], H_2 [2–5], CH_4 [6–9] or other hydrocarbons [10]). These characteristics make it a promising candidate as a technology for the storage of electrical energy from renewable, intermittent sources into chemical energy. The exploitation of these potentialities towards actual industrial utilization requires research efforts devoted to both a substantial increase in the energy efficiency and selectivity of the process towards value-added products. Almost all kinds of discharges at atmospheric pressure have been tested to this purpose: dielectric barrier (DBD) [2, 3, 6, 7, 9], microwave [1,5], Glide-Arc [8], Corona [10,11]. Recently, we have tested a nanosecond repetitively pulsed discharge (NRP) in a CO_2-CH_4 mixture, finding encouraging energy efficiency and selectivity towards syngas formation [12]. Although the discharge design was a pilot first approach one, without any optimization effort to match the discharge geometry with the gas flux, we obtained energy conversion efficiencies among the highest found in the literature for all the other kinds of discharge. The actual investigation approach to plasma conversion issues relies on: a) technological efforts devoted to discharge design and, eventually, coupling with heterogeneous catalysis systems; b) measurement of stable products in the gas downstream by chemical analytical techniques (e.g. chromatography, mass spectrometry and FTIR spectroscopy) [13]; c) computer modelling of the plasma chemistry [14]; d) comparison between experimental and computational results to improve the initial discharge design [9]. The experimental investigation of discharge kinetics can be pursued by time resolved diagnostics of both transient and stable species. Laser induced fluorescence is well suited to this aim, due to its spatial and temporal resolution [15]. Among transient species, the hydroxyl radical, whose reactivity can be of great importance in the kinetics of any plasma-chemistry process, may have a role also in the present issue. The presence of water in a discharge leads to the production of OH. Water is frequently found in CO_2 plasma conversion, either as a part of the initial mixture or as a process product. H_2O can be added to the mixture as a cheap and abundant hydrogen source, and it is unavoidably present, together with CO_2, in industrial waste gas or biogas. Even in the CO_2 + CH_4 dry

reforming, water is a by-product [12]. In an industrially meaningful plasma CO_2 conversion, the chemical kinetics must then cope with the presence of water and, then of the OH radical. OH might be detrimental for CO_2 conversion, due to the fast (rate constant $1.57 \times 10^{-13}\,\mathrm{cm^3\,s^{-1}}$ at T = 400 K [16]) reaction

$$\mathrm{CO + OH \rightarrow CO_2 + H} \tag{1}$$

such that in a CO_2+H_2O dielectric barrier discharge, this reaction has been indicated as a limiting factor for conversion [14]. On the other hand, OH can add to CO to form COOH:

$$\mathrm{CO + OH \rightarrow COOH} \tag{2}$$

with a rate constant, estimated in [6], of $1.5 \times 10^{-12}\,\mathrm{cm^3\,s^{-1}}$. The COOH radical is an intermediate in the pathway leading to carboxylic acids (e.g. formic, acetic, propanoic and butanoic acid). This is then a case in which the kinetics of a transient specie can be determinant for the final products and conversion efficiency. It is then worth to investigate both OH density and its time evolution in the discharge and post-discharge phases. The time evolution compared with rate coefficients of possible reactions involving OH, helps to understand its effective role in the conversion process.

Stable species also can be monitored by time-resolved diagnostics to investigate their formation kinetics and their history in the discharge. Such a knowledge can be useful not only to understand the mechanism but also to optimize the discharge energy expenditure, rather than relying only on the final concentration result. In the specific case of CO_2 conversion, the time evolution of the gas composition might be investigated, for example, monitoring CO by Two-photons LIF (TALIF) [17]. A further possibility will be proposed here.

The present work deals with the application of OH LIF measurements to a nanosecond repetitively pulsed discharge. Several issues of the LIF methodology and the physical characteristics of an NRP must be addressed and solved to this aim. In particular the rapidly changing conditions of temperature, gas density and composition determine a hostile environment for a quantitative LIF application. The first part of the paper is devoted to a detailed description of such a set of problems and the routes to their solution. In this frame, we establish a methodology which we may call CET-LIF (Collision Energy Transfer LIF), by which we aim at using OH LIF outcomes to investigate the gas composition, and in particular CO_2 dissociation,

even in the difficult conditions of an NRP discharge. Some results are then reported with the aim of showing different conditions of LIF application and its potentiality for discharge kinetics studies.

2. Problem overview

2.1. LIF and collision energy transfers

The LIF principles and application to atmospheric pressure discharges are detailed in a previous publication [15]. Here we recall them briefly and underline the issues relevant to the paper content. Starting from the classical LIF scheme for OH detection (according to Hund's case b notation):

$$\begin{array}{l} \mathrm{OH}(X,0,N'') + h\nu_L \rightarrow \mathrm{OH}(A,1,N') \rightarrow \mathrm{OH}(X,1) + h\nu_{(1,1)} \\ \qquad\qquad\qquad\qquad \downarrow {\scriptstyle VET} \\ \qquad\qquad\qquad\qquad \mathrm{OH}(A,0) \rightarrow \mathrm{OH}(X,0) + h\nu_{(0,0)} \end{array} \tag{3}$$

The first step is the absorption of a photon by a ro-vibronic transition. With common dye laser bandwidths, of the order of $0.2\,\mathrm{cm}^{-1}$, it is easy to tune the wavelength to a single line (typical line widths are around $0.15\,\mathrm{cm}^{-1}$ at 760 Torr, 400 K), such that light absorption causes overpopulation of a single rotational level N', and a single spin-orbit sublevel (F_1 or F_2).

The fluorescence light emitted by the excited OH(A) state is the measurable quantity. In particular two outcomes can be recorded: a) time-resolved spectrally-integrated LIF signal (LIF pulse); b) spectrally-resolved time-integrated fluorescence spectrum (LIF spectrum). In a collisionless environment, only radiative de-excitation occurs, and emissions of branches originating from the excited sublevel (N', F) only can be observed. Collisional environments introduce three kinds of energy exchanges. Rotational energy transfers (RET) mix the populations of rotational levels in a given vibro-electronic state. Such a mixing determines the appearance of fluorescence from rotational levels other than the single sublevel populated by the laser, up to a limit case in which a fully thermalized rotational distribution is quickly achieved and observed in the fluorescence spectrum. The second kind of energy exchange is electronic quenching, Q, i.e. the collisional depopulation of the vibro-electronic state with accommodation of its energy out of the electronic state. Q has a large influence on the vibro-electronic state lifetime and its importance is twofold. First, it determines the total number of fluorescence photons available

to the detection, in other words, the LIF signal magnitude. Second, it rules the possibility of rotational population redistribution. This latter in fact depends on the number of RET collisions within the state lifetime. In practice, since RET and Q frequencies depend linearly on the bath gas density, the degree of rotational redistribution depends on the rate coefficients ratio k_{RET}/k_Q, and is independent of the gas density itself. Both RET [18, 19] and Q [20, 21] rate coefficients depend on the rotational level. Q rate coefficients are also strongly dependent on the bath gas molecular components [22].

A further step occurs, in the specific case of scheme 3 for OH, due to the third kind of collision process, the vibrational energy transfer (VET), i.e. the exchange among vibrational levels of the same electronic state. VET relaxation from $v' = 1$ to $v' = 0$ generates fluorescence from the lower vibrational level also. VET rate coefficients are also strongly dependent on the bath gas molecular components [22]. As a whole, then, the observable quantity is the fluorescence from both levels. In particular, for practical reasons, from the (1,1) and (0,0) bands of the 3064 Å system, respectively, that are the most intense ones and occur such close to each other as to be collected in a single spectral window of the spectrometer.

A quantitative analysis of the LIF outcome then requires a knowledge of the gas composition and density, of the rate coefficients of the collision processes, and a rate equation model as described in detail in [15]. Since the rate coefficients depend on the rotational level, the knowledge of the rotational distribution of the OH(A) state is necessary for the assessment of an effective rate coefficient. In a collisional environment, one limit case can be defined only, i.e. that of thermal equilibrium with the bath gas, that is achieved at any time along the fluorescence decay provided $k_{RET}/k_Q \gg 1$. In such a case the effective rate constant of a given collisional process corresponds to that of a thermalized rotational distribution, such that the rate constant of a vibro-electronic level can be formally defined (together with its dependence on the gas/rotational temperature, see [23]). In practice, the effective "equilibrium" rate constant is determined by the rotational levels which have the larger rate constants. The $k_{RET}/k_Q \gg 1$ condition is typically met in atmospheric pressure plasma jets (APPJ), in which generally small percentages of molecular gases, nitrogen, water, oxygen, are carried in a large flux of He or Ar. Both carrier gases, He in particular, feature large k_{RET} values against small k_Q ones, while the small molecular gas amount keeps low the total quenching frequency value. He carrier gas has been used in [22] where Q and VET rate constants for many

molecular colliders have been measured for a Boltzmann rotational distribution at 300 K. Pure molecular mixtures, on the contrary, show almost opposite behaviour. Very large quenching rate constants determine a condition for which $k_{RET}/k_Q < 1$. The observed fluorescence spectra of the (1,1) band preserve a clear memory of the nascent distribution, with small contributions from close rotational levels. Sample spectra in molecular gases are shown in Figure 1.

The spectra have been measured in a cell at room temperature, with the addition of water peroxide vapour to the pure molecular gas, to get OH from H_2O_2 photodissociation as in [22]. These are preliminary data, and the simulated spectrum is not a fit but just a visual match obtained by setting manually the rotational population distribution. More accurate results require much higher spectral resolution: work is in progress along this improvement. Nevertheless, we can recognize a 'quasi' nascent rotational distribution of $v' = 1$, and a distributed rotational excitation of $v' = 0$, that in the figures has been simulated by a Boltzmann distribution. 'Quasi' nascent means a prevalent population of the rotational level excited by the laser and a smaller population of nearby levels. Such a simulation is not accurate, but shows clearly that the VET relaxation leaves the $v' = 0$ state with a supra-thermal rotational excitation, here exemplified by a temperature, and that such a distribution depends on the collider gas, as already reported in [21].

We have investigated laser excitation of $J' = 0.5 - 4.5$ through wavelength tuning from $P_1(1)$ (2821.70 Å) to $P_1(5)$ (2839.45 Å), finding 'quasi' nascent rotational distribution of v'=1 relevant to the excited rotational level, and $v' = 0$ rotational distribution that, within the accuracy level of these measurement, do not appear to depend on the excited J' level. Analogously, the VET rate coefficient, at first sight, do not depend on the excited J', and their value seems to be very close to the 'thermal' one measured in [22]. Deeper investigations are needed that will rely on highly resolved fluorescence spectra.

2.2. NRP discharges

Nanosecond repetitively pulsed discharges have only recently been applied to the CO_2 conversion issue, but they have been the subject of many investigations in the last two decades in the frame of plasma assisted combustion. The most recent observations on pin-to-pin NRP at atmospheric pressure [25, 26] depict a hostile environment for LIF diagnostic application. In the spark regime, a hot kernel in

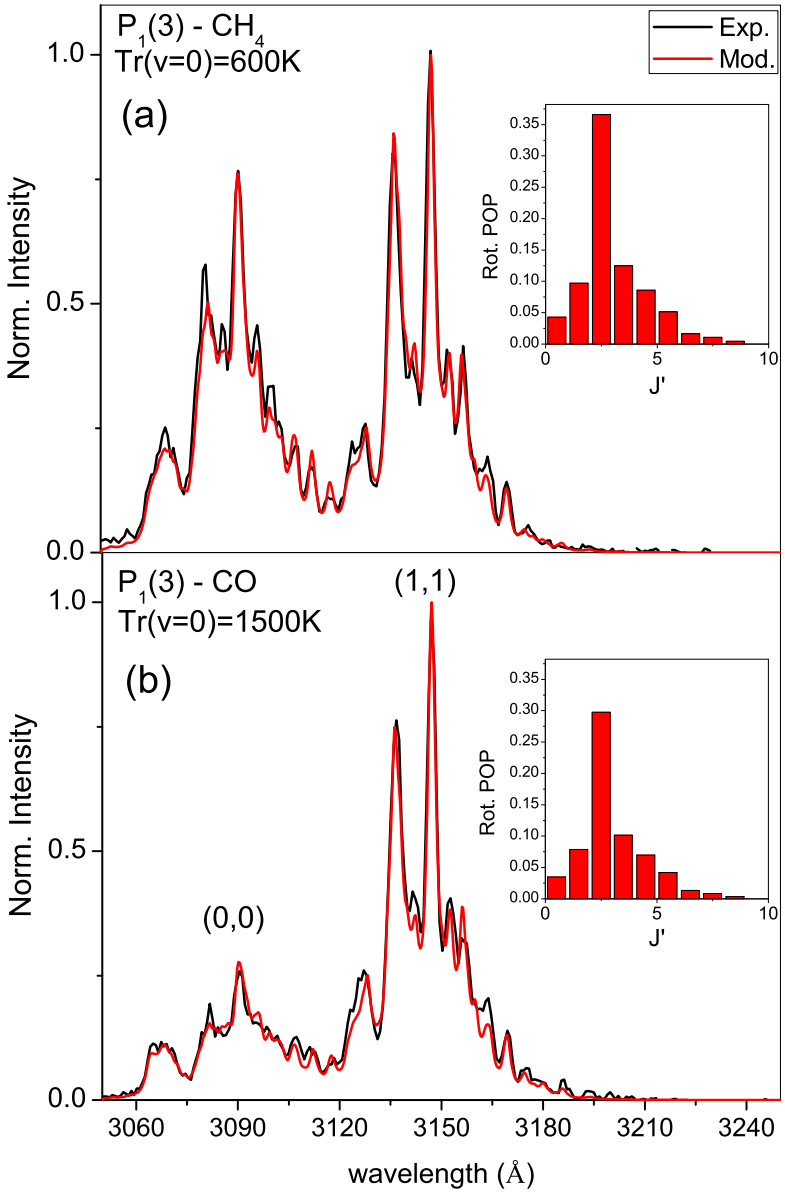

Figure 1. Fluorescence spectra in 8 Torr of CH_4 (a) and CO (b), with about 0.1 Torr of H_2O_2 + H_2O, with laser tuned to the $P_1(3)$ line. Excitation of the rotational level $N' = 2$, sublevel F_1', i.e. $J' = 2.5$. Simulations are calculated by LIFBASE [24]. In the inset figures the rotational distribution of $v' = 1$, that approximately reproduces the observed spectrum. The $v' = 0$ rotational distribution of the simulated spectrum is a Boltzmann one, with a temperature specified in the figure.

the discharge filament with high gas temperature, more than 2000 K, is formed, followed by expansion and cooling also due to gas recirculation, in the tens of µs time scale. Such an 'explosive' behaviour generates a collisional environment for LIF outcomes with unknown and rapidly changing gas density. In addition, the gas mixture composition also drastically changes due to the huge molecular dissociation. For these reasons, even if the relevant rate coefficients are known, it is not possible to determine apriori the Q and VET frequencies. A way out could be to determine the frequencies from the measured fluorescence spectrum and pulse fitted, as in [15], by the rate equation model. In the specific case of CO_2 conversion, with CO, CH_4, O_2 H_2 as other gas species involved, however, the quenching rate constants are huge [22]. In pure CO_2, for example, $k_{Q0} = (45.5 \pm 1.1) \times 10^{-11} \mathrm{cm}^3\,\mathrm{s}^{-1}$ and $k_{Q1} = (61.4 \pm 3.5) \times 10^{-11} \mathrm{cm}^3\,\mathrm{s}^{-1}$ for $v' = 0$ and $v' = 1$ respectively. The quenching frequency at ATP is then around $1.5 \times 10^{10}\,\mathrm{s}^{-1}$. A LIF measurement of the collision frequencies therefore requires the use of ps tunable lasers and a fast detector, like a streak camera.

With conventional ns lasers and detectors there is still room for kinetic investigations by LIF. One possibility is a 'soft' discharge approach, in which the explosive nature of an NRP with metallic electrodes is mitigated by the insertion of a dielectric layer above one of the electrodes, i.e. an NRP-DBD. In such a case the gas temperature remains low, despite a still remarkable discharge energy/pulse of some mJ.

A further possibility is to take advantage of the knowledge on collision processes to extract useful information from ns-LIF, even in a hostile environment, as it is detailed in the next paragraph.

2.3. Collisional LIF

The simultaneous recording of LIF spectra and pulses, both including the two (0,0) and (1,1) bands, allows the determination of VET and Q frequencies. If the collisional rate coefficients are known for the environment molecules, the densities of gas components can be determined from the measured frequencies. This use of LIF outcomes was demonstrated in [27] to be possible in He/Ar + air + water mixtures and applied to an APPJ for plasma medicine applications in [15, 28, 29] for the independent determination of air and water penetration in the effluent jet. The basis of this method relies on the occurrence of sharp differences in the collisional

rate coefficients for different molecules. For example, water is a very fast quencher but a slow VET source, while nitrogen has an opposite behaviour. In CO_2 conversion mixtures, remarkable differences also exist. As it is evident from the relative emission of (0,0) and (1,1) bands in Figure 1, remarkably less VET is induced by CO than by CH_4. Looking at the rate coefficients reported in Table 1 of [22], a significant CO_2 dissociation into CO and O_2 clearly produces a lowering of the VET efficiency and then a corresponding lower (0,0) and (1,1) band emission ratio, as it is shown in the following.

We underline that the band ratio in the fluorescence spectrum depends only on the VET over Q_0 frequencies ratio. Since both frequencies depend linearly on the gas density, the ratio is independent of the gas pressure and temperature conditions and is determined only by the rate coefficients ratio k_{VET}/k_{Q0}. In addition, the fluorescence measurement is time integrated, and it does not require high time resolution in presence of very fast quenching. In other words, the time integrated fluorescence bands ratio depends only on the gas mixture composition (gas components molar fractions) and, in simple initial mixture cases, it can be used to extract information on the CO_2 dissociation even in a hostile environment like that of a NRP.

We deduce the gas composition by using the numerical analysis reported in [22] for the measurement of collision rate coefficients, and the reader can refer to that paper for technical details. In summary, the LIF process is modelled by the 5-level scheme described in [15]. The system of rate equations for the populations of the levels is solved numerically, and the solution is fitted to the LIF outcomes through a numerical algorithm with the VET and Q frequencies as parameters. The band emission ratio is also used as an input parameter and it is calculated by fitting a LIFBASE [24] simulation to the spectrally resolved experimental data (similar to those of Figure 1). Since the VET and Q rate coefficients for the various gases are known, the VET and Q frequencies are used to determine the gas composition. In the specific case of a CO_2+H_2O mixture, the major gas components are CO_2, CO, O_2 and H_2O. The LIF pulse decay cannot be measured, absolute collision frequencies cannot be deduced, but only the k_{VET}/k_{Q0} is available from the band ratio. As said before this is sufficient to infer the relative gas components amounts (i.e. the mixture composition), even if the total gas density in unknown.

We might call this methodology Collisional Energy Transfers LIF (CET-LIF) since it is based on the use of quantified collisional processes involving the electronic state pumped by laser absorption. Note that in CET-LIF the molecule on which the

LIF is performed is just a 'probe' molecule. The present case of OH is a favourable one since collision processes for OH$(A, v = 0, 1)$ are quite well characterized, and since the spectroscopic features of OH make it a suitable molecule for this kind of studies. Other molecules could be used as well, provided a detailed set of collisional rate coefficients is available. Finally we observe that another appropriate name could be LCIF (Laser Collision Induced Fluorescence), but this name is actually associated to the particular case of energy transfers by electron collision only [30].

3. Experimental

The setup for LIF measurements is the same as that reported in detail in [15]. We shall not describe it here for the sake of brevity. The discharge apparatus is schematically shown in Figure 2. The electrodes assembly is placed into a vacuum tight quartz chamber equipped with three arms and windows for laser beam passage and fluorescence collection. The two electrodes are made of a 1 mm diameter tungsten rod with a sharpened edge. The HV electrode is covered by a quartz tube with 2 mm internal diameter. The gas flows within the tube and around the tungsten rod. The grounded electrode is an identical sharpened rod, that, in the DBD configuration is covered by a 8 mm diameter macor rod with a 1.5 mm thickness at the electrode tip.

The HV nanosecond-scale pulses are produced by a Megaimpulse NPG 18/3500 generator, triggered by a wave-form generator. The pulses pattern is made of pulse bursts repeated at a frequency of 10 Hz, each burst being composed of 10 pulses at a frequency of 3 kHz. I.e., a burst is composed of ten discharge events separated by a 333 µs time interval. A closer pulse spacing in the burst is not possible with the present HV generator. The pulse pattern is shown in Figure 3. A further 100 Hz pulse pattern is superimposed in such a way that a pre-pulse always precedes by 5 ms the burst. This ensures that the first voltage pulse of the burst always produces a discharge.

The discharge current and voltage values are measured by a Magnelab CT-D-1.0 I/V converter (Bw=500 MHz) and a Tektronics P6015A probe (Bw=75 MHz), respectively. V/I signals are recorded by a LeCroy HDO9104 digital oscilloscope. Water is transported into the chamber by a gas fraction flowing through a temperature controlled bubbler. Mass-flow controllers regulate the gas inlet.

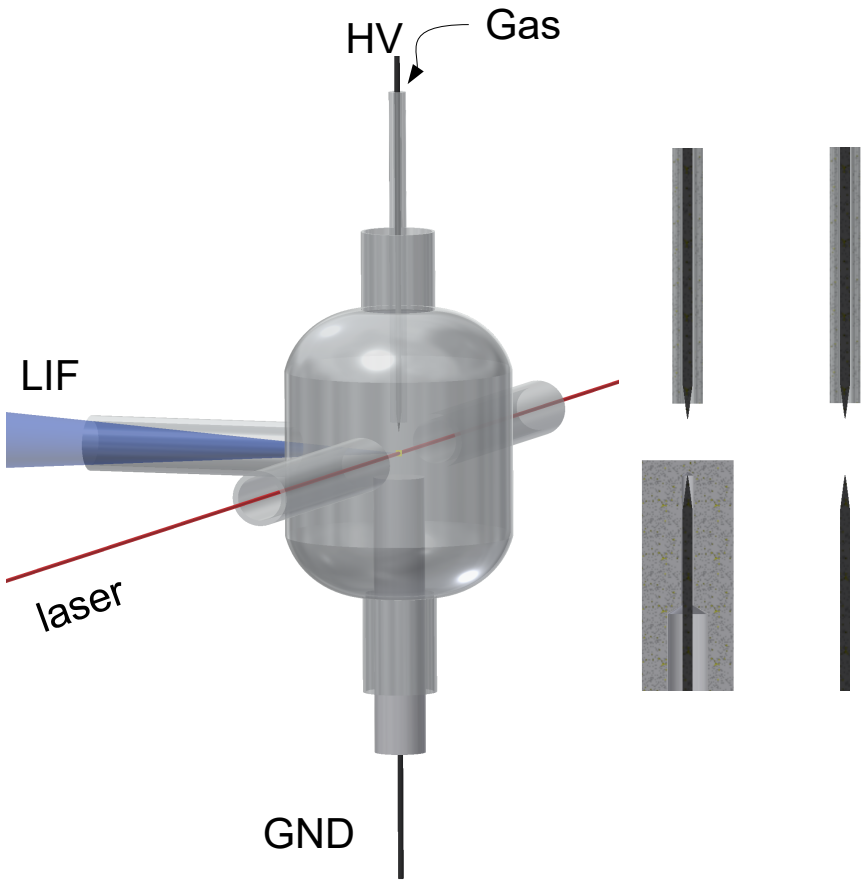

Figure 2. Drawing of the discharge cell with the three arms for LIF implementation and the two electrodes feedthroughs. The sectional drawing of the electrodes assembly is shown also, with and without the macor cap for the DBD-NRP and simple NRP respectively.

4. Results and Discussion

We present sample results obtained in three CO_2+H_2O discharge configurations, ordered according to an increasing degree of difficulty in the application of LIF: a) a DBD discharge in He buffer gas; b) a NRP discharge in He buffer gas; c) a NRP discharge without buffer gas. The visual appearance of the three discharge kinds is shown in Figure 4.

In case a), the presence of He ensures: 1) rotational thermalization of the OH(A)

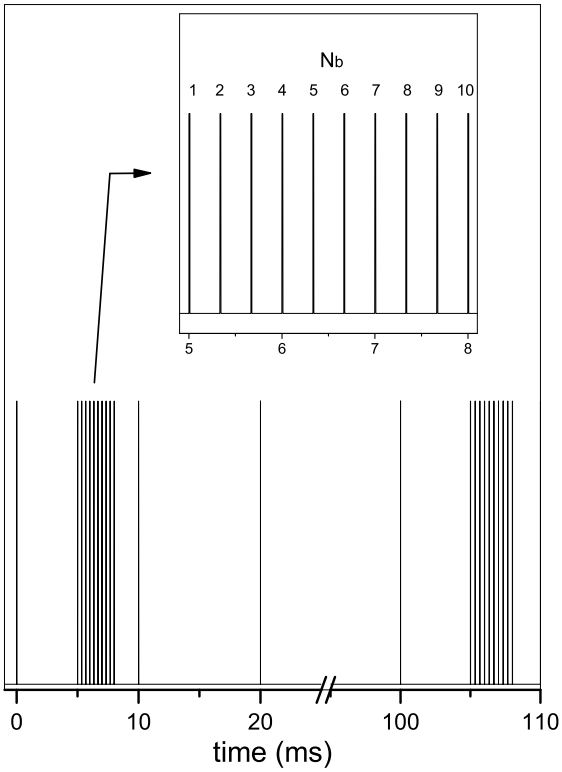

Figure 3. The temporal pattern of discharge voltage pulses. The pattern within the burst is shown in the inset with enlarged time scale and the single pulses labelled with progressive numbers N_b.

state such that the rate coefficients of [22] can be used; 2) the small molecular gas content keeps low the quenching frequency, that can be measured from the fluorescence pulse decay. The collision processes involving $OH(A, v = 0, 1)$ can then be fully quantified. The DBD configuration, in turn, ensures a large discharge volume (see Figure 4a), i.e. the LIF sampled volume is well defined by the laser beam geometry, and a low gas temperature, measured by LIF excitation spectrum, ranging between 300 K and 350 K. In this case, OH densities can be measured. CET-LIF can be applied as well to investigate the gas composition.

In case b), again the collision processes can be well characterized thanks to the He buffering, and the discharge size (Figure 4b) is similar to that of the laser beam. The OH concentration can still be measured and CET-LIF is applicable.

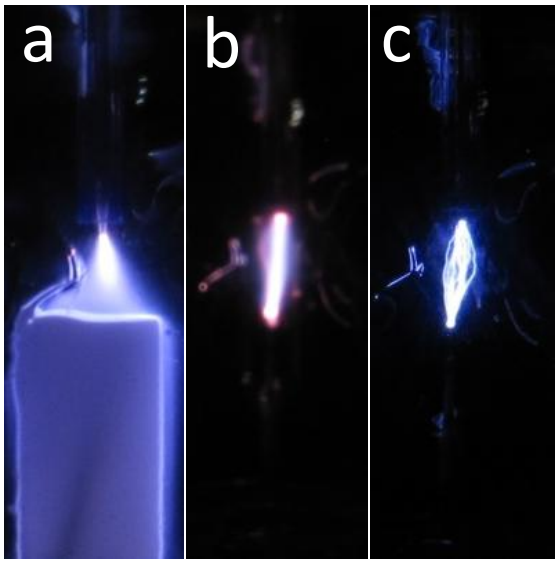

Figure 4. Pictures of a) NRP-DBD in He-CO_2-H_2O; b) NRP in He-CO_2-H_2O; c) NRP in CO_2-H_2O. The camera exposure time is enough long as to capture altogether the ten pulses of a burst.

In case c) quenching frequencies are not measurable. The discharge is explosive and thin, and successive discharges in the burst do not fill the same volume, as shown in Figure 4c. The collisional environment cannot be characterized, so that the OH concentration cannot be measured, neither absolutely nor relatively. CET-LIF only can be applied.

The measurements within the burst are made at variable delays with respect to a single pulse (N_b). The aim is to monitor the evolution of the OH concentration and CO_2 dissociation after the pulse and to look for possible build-up effects on these quantities after successive pulses of the burst. The total gas flow is 150 sccm, that implies a minimum time for crossing the 5.2 mm discharge gap of about 4.45 ms. Given that the laser beam is positioned at 3.7 mm from the electrode tip, the monitored volume is a region where the flowing gas can see up to ten pulses of the burst. Strictly inside the discharge, the LIF signal is overwhelmed by plasma emission, such that time resolved scans start from a delay of 2 µs, where the level of plasma emission is low enough to be safely subtracted. The [OH] time evolution is measured by fixed laser wavelength tuned to the $Q_2(3)$ transition.

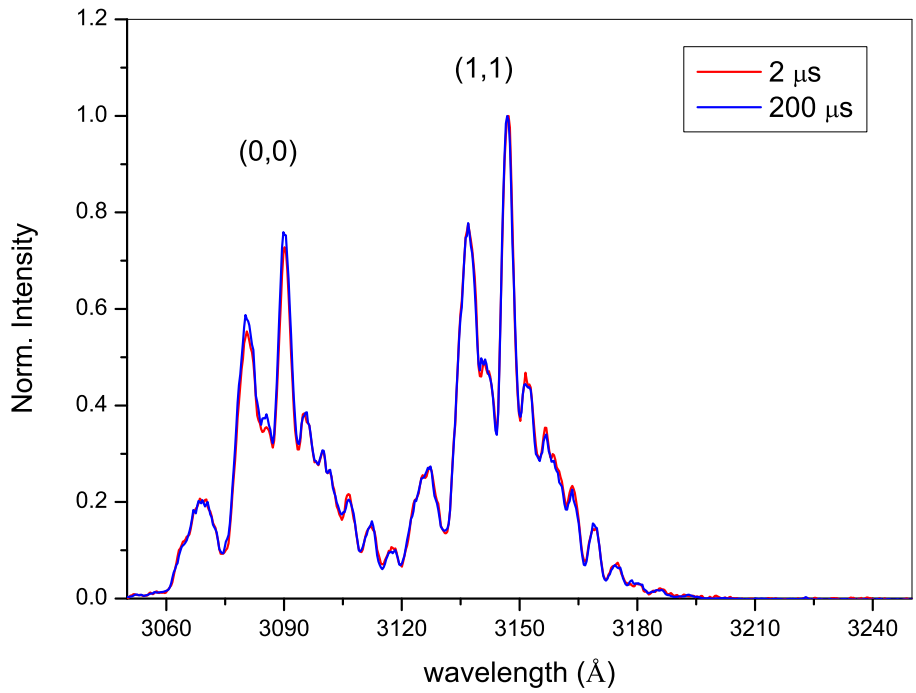

Figure 5. Fluorescence spectra in the NRP-DBD with He buffer gas, at two delays in the first after-pulse (N_b=1). He+ 4 Torr CO_2 + 0.75 Torr H_2O. E_{disch}=10.8 mJ pulse^{-1}.

4.1. NRP-DBD in He-CO_2-H_2O

Two gas mixtures have been investigated: (1) 2 Torr CO_2 + 2 Torr H_2O and (2) 4 Torr CO_2 + 0.75 Torr H_2O, both at a total pressure of 760 Torr with He buffer gas. The fluorescence spectrum reported in Figure 5 shows a thermalized rotational distribution. The time evolution of OH concentration is reported in Figure 6 (green diamonds for mixture (1), blue triangles for mixture (2)). A fast initial decay, with time constant of about 11 and 14 µs for mixtures (1) and (2) is observed, followed by a very slow further decay. In mixture (1) the OH density is quite larger than in mixture (2), due to the larger amount of water.

The band ratio in the gas mixture (1) does not show appreciable CO_2 dissociation, while in the mixture (2), and at a doubled energy/pulse (E_{disch}=10.8 mJ pulse^{-1}), Figure 5, the LIF spectrum can be fitted allowing for a small CO_2 dissociation. In the hypothesis that the dominant final products are just

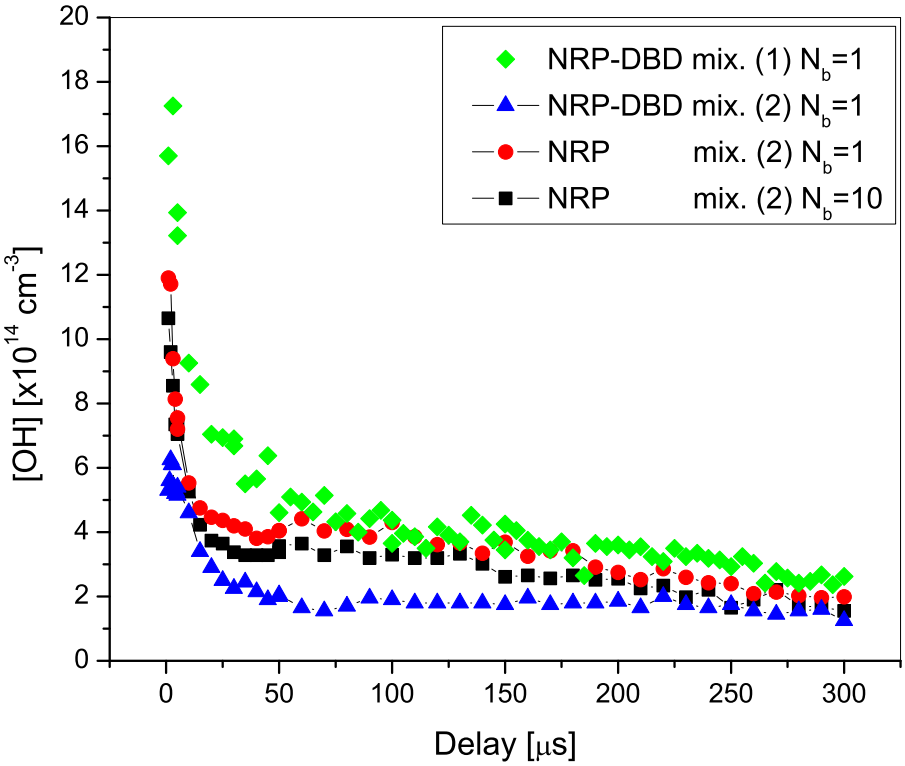

Figure 6. OH concentration and decay in the after-pulse. Green: NRP-DBD, mixture (1), E_{disch}=4.1 mJ pulse^{-1}; blue: NRP-DBD, mixture (2), E_{disch}=4.7 mJ pulse^{-1}; red and black: NRP, mixture (2), E_{disch}=5.7 mJ pulse^{-1}, N_b=1, 10 respectively.

CO and O_2, the spectrum at 2 µs can be fitted by assuming a 14% CO_2 dissociation. This value goes down to about 5% within the first 200 µs and then remains almost constant. It is clear from the figure that these values are at the limit of CET-LIF detectability, and must be taken as indicative. The dissociation values and behaviour in the after-pulse time have been nevertheless observed at every pulse, so that we can report that no build-up effect is observable at successive pulses in the burst.

4.2. NRP in He-CO_2-H_2O

The removal of the Macor cap produces some changes in the discharge kinetics. The [OH] decay in the gas mixture (2), reported in Figure 6 (red circles and black squares

for the data recorded after $N_b = 1$ and $N_b = 10$, respectively) has a similar trend as the corresponding one in the (NRP-DBD), but a faster initial decay. Changes from the first to the tenth pulse are also minimal. The same holds for LIF spectra, with approximate CO_2 dissociations of the same order of magnitude. The initial [OH] decay has, in both N_b cases of Figure 5, a time constant of 4-5 µs. Reaction 2 cannot account for such a fast decay. In fact the band ratio in LIF spectra is compatible with dissociations of the order of 10%, i.e. a CO density of $1.3 \times 10^{16}\,\mathrm{cm}^{-3}$, giving an OH decay time constant by reaction 2 of about 50 µs. Other mechanisms must be then looked for to explain the [OH] decay, unless we put into question the rate constants of reactions 1 and 2. On the other hand, with this CO concentration, and an OH density one order of magnitude lower, reactions 1 and 2 do not appear to be a major CO loss mechanism.

These few preliminary results then do not support an important OH role in CO back reactions in the present conditions. On the other hand, the measurements must be refined and performed in more favourable conditions. Here we limit to point out the potential of this kind of diagnostic investigation in revealing the underlying chemical kinetics of NRP discharges.

4.3. NRP in CO_2-H_2O

Spectra recorded in the first after-pulse are shown in Figure 7. The initial gas mixture is CO_2 + 11.25 Torr H_2O. The band ratio at short delay times appears to be dramatically different from that of undissociated CO_2 environment. Using the 'thermal' rate coefficients, the spectra in the figure are fairly well reproduced at a dissociation of 67% and 15% at 10 and 200 µs respectively. Again these values must be considered as indicative, but not that far than the true ones. According to spectra measured in the absence of a discharge, the k_{VET}/k_{Q0} ratio does not appear to be much different from the 'thermal' case, but an error in the dissociation yield may come from an imperfect fit of the non-equilibrium rotational distributions. It is nevertheless clear that a huge amount of CO_2 is dissociated, and that this happens in a single discharge pulse. No build-up is in fact observed up to the last pulse of the burst, being this at least partly attributable to the discharge geometry, such that successive pulses do not cross the same volume. However, the relative amount of CO_2 increases much in the after-pulse time, in a time scale that is compatible with fluid dynamic remixing of 'discharged' gas with the untreated volume [25]. Of course

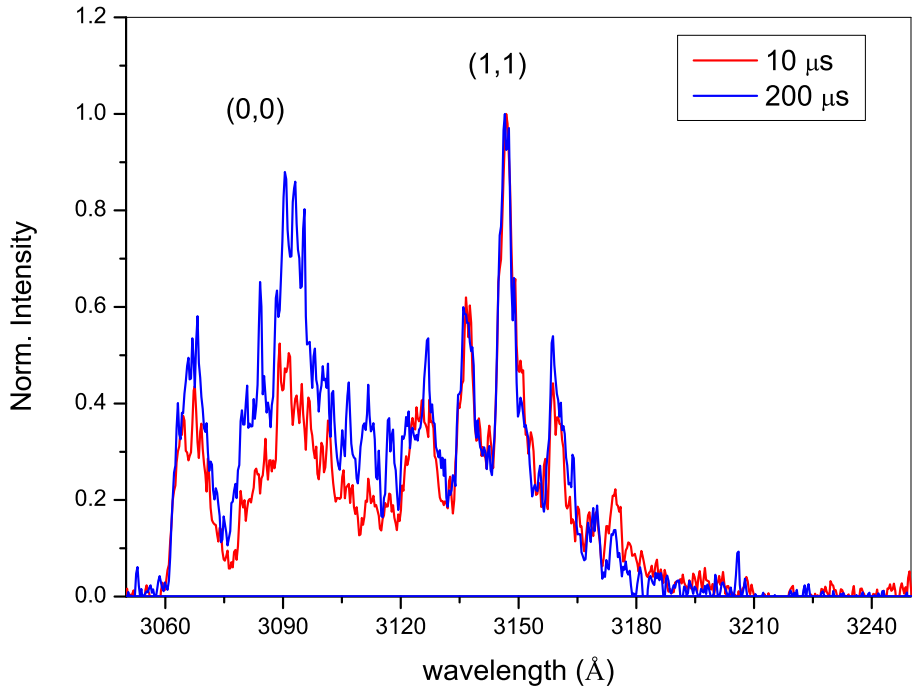

Figure 7. Fluorescence spectra in the CO_2 NRP, at two delays in the first after-pulse. Gas mixture (2), E_{disch}=2.9 mJ pulse^{-1}. Laser excitation of the $J' = 2.5$ rotational level ($Q_2(3)$ line).

other chemical routes cannot be excluded. The significant dissociation increase with respect to the He buffered mixture could be due to the much larger discharge energy density, since the energy is deposited in a much smaller volume. This is confirmed by the local gas temperature, measured by LIF excitation spectra as in [15], that is about 2300 K close to discharge and drops to about 800 K at a delay of 200 µs. Such a quick cooling is probably due to the gas expansion and recirculation described in [25].

5. Conclusions and outlook

In summary, discharges with He dominant specie in the gas mixture are suitable for fully quantitative application of LIF. Although these discharges do not produce significant CO_2 dissociation, they are very much attractive for the understanding of kinetic mechanisms. One possible improvement concerns the observation that

no build-up of species is found along the pulse time series in the burst and the possibility that this might be due to the temporal distance between the pulses being much larger than the decay time of the species. It will be worth investigating a substantial shortening of this delay. On the other hand, the removal of He buffer gas presents a much more interesting configuration for applicative purposes, with very high dissociation yields in a single pulse. In addition, since at the actual repetition rate no build-up is observed for CO_2 dissociation, and the discharge does not appear to fill the entire volume, for the purpose of a large and efficient CO_2 conversion, the technological challenge should follow two directions: a) not that much to increase the pulse energy or the number of pulses in the same volume, but rather to fill most of the gas volume with single pulses; b) find a way to freeze the dissociation at the high values found in the early after-pulse, at least for that part of dissociation decrease in the after-pulse eventually due to back reactions. Further studies, in more controllable discharge geometries, will try to clarify the role of fluid dynamic remixing and back reactions in the after-pulse kinetics.

From a diagnostic point of view, that is the core business of the present paper, we have shown that, even in hostile conditions, CET-LIF is applicable and can provide crucial information. The step towards a fully quantitative application of CET-LIF in the CO_2 NRP is the detailed measurement of the rotational distributions in the OH(A) state and the collision rate constants in non-equilibrium conditions. It is also clear that a fully quantitative LIF application for OH absolute concentration measurements (as well as for other species), in the NRP discharge without He buffering, requires a technological improvement towards picosecond scale time resolution of lasers and detectors.

Acknowledgments

L.M. Martini acknowledges financial support from Fondazione Cassa di Risparmio di Trento e Rovereto, Grant Bando 2016 per progetti di ricerca scientifica svolti da giovani ricercatori post-doc.

6. References

[1] Chen G, Silva T, Georgieva V, Godfroid T, Britun N, Snyders R and Delplancke-Ogletree M P 2015 *International Journal of Hydrogen Energy* **40** 3789 – 3796

[2] Eliasson B, Kogelschatz U, Xue B and Zhou L M 1998 *Industrial & Engineering Chemistry Research* **37** 3350–3357

[3] Zeng Y and Tu X 2016 *IEEE Transactions on Plasma Science* **44** 405–411

[4] Jwa E, Lee S, Lee H and Mok Y 2013 *Fuel Processing Technology* **108** 89 – 93 special Issue of APCRE11

[5] de la Fuente J F, Moreno S H, Stankiewicz A I and Stefanidis G D 2016 *International Journal of Hydrogen Energy* **41** 21067 – 21077

[6] Martini L M, Dilecce G, Guella G, Maranzana A, Tonachini G and Tosi P 2014 *Chem. Phys. Lett.* **593** 55 – 60

[7] Scapinello M, Martini L M and Tosi P 2014 *Plasma Process. Polym.* **11** 624–628

[8] Tu X and Whitehead J C 2014 *Int. J. Hydrogen Energy* **39** 9658 – 9669

[9] Snoeckx R, Zeng Y X, Tu X and Bogaerts A 2015 *RSC Adv.* **5**(38) 29799–29808

[10] Zhang X, Zhu A, Li X and Gong W 2004 *Catalysis Today* **89** 97 – 102

[11] Li M w, Xu G h, Tian Y l, Chen L and Fu H f 2004 *The Journal of Physical Chemistry A* **108** 1687–1693

[12] Scapinello M, Martini L M, Dilecce G and Tosi P 2016 *J. Phys. D: Appl. Phys.* **49** 075602

[13] Pinhão N, Moura A, Branco J and Neves J 2016 *International Journal of Hydrogen Energy* **41** 9245 – 9255

[14] Snoeckx R, Ozkan A, Reniers F and Bogaerts A 2017 *ChemSusChem* **10** 409–424

[15] Dilecce G, Martini L M, Tosi P, Scotoni M and De Benedictis S 2015 *Plasma Sources Sci. Technol.* **24** 034007

[16] Baulch D L, Cobos C J, Cox R A, Esser C, Frank P, Just T, Kerr J A, Pilling M J, Troe J, Walker R W and Warnatz J 1992 *J. Phys. Chem. Ref. Data* **21** 411–734

[17] Mosburger M and Sick V 2010 *Appl. Phys. B* **99** 1 – 6

[18] Kienle R, Jorg A and Kohse-Hoinghaus K 1993 *Appl. Phys. B* **56** 249 – 258

[19] Kienle R, Lee M P and Kohse-Hoinghaus K 1996 *Appl. Phys. B* **63** 403 – 418

[20] Copeland R A, Dyer M J and Crosley D R 1985 *J. Chem. Phys.* **82** 4022–4032

[21] Copeland R A, Wise M L and and D R C 1988 *J. Phys. Chem.* **92** 5710

[22] Martini L M, Gatti N, Dilecce G, Scotoni M and Tosi P 2017 *J. Phys. D: Appl. Phys.* **50** 114003

[23] Tamura M, Berg P A, Harrington J E, Luque J, Jeffries J B, Smith G P and Crosley D R 1998 *Combust. Flame* **114** 502 – 514

[24] Luque J and Crosley D 1999 *SRI Int. Rep. MP 99-009*

[25] Castela M, Stepanyan S, Fiorina B, Coussement A, Gicquel O, Darabiha N and Laux C O 2017 *Proceedings of the Combustion Institute* **36** 4095 – 4103

[26] Lo A, Cessou A, Lacour C, Lecordier B, Boubert P, Xu D A, Laux C O and Vervisch P 2017 *Plasma Sources Sci. Technol.* **26** 045012

[27] Dilecce G 2014 *Plasma Sources Sci. Technol.* **23** 015011

[28] Riés D, Dilecce G, Robert E, Ambrico P, Dozias S and Pouvesle J M 2014 *J. Phys D: Appl. Phys.* **47** 275401

[29] Martini L M, Maranzana A, Tonachini G, Bortolotti G, Scapinello M, Scotoni M, Guella G, Dilecce G and Tosi P 2017 *Plasma Processes and Polymers* Doi: 10.1002/ppap.201600254

[30] Barnat E V and Frederickson K 2010 *Plasma Sources Sci. Technol.* **19** 055015